Contents lists available at ScienceDirect

The Egyptian Journal of Remote Sensing and Space Sciences

Research Paper

Estimation of above ground biomass of mangrove forest plot using terrestrial laser scanner

Yeshwanth Kumar Adimoolam [a], Nithin D. Pillai [b], Gnanappazham Lakshmanan [c,*],
Deepak Mishra [c], Vinay Kumar Dadhwal [d]

[a] *CYENS Center of Excellence, Cyprus*
[b] *GFZ Helmholtz Centre, Potsdam, Germany*
[c] *Indian Institute of Space Science and Technology, Valiamala, Trivandrum, India*
[d] *National Institute of Advanced Studies, Bangaluru, India*

ARTICLE INFO

ABSTRACT

Above-Ground Biomass (AGB) is an important parameter in the conservation of mangrove ecosystem owing to their ecological and economic benefits. LiDAR technologies in forest studies have become popular, due to its highly accurate 3D spatial data acquisition. In this study, we propose an end-to-end framework for estimating AGB of mangroves from Terrestrial Laser Scanner (TLS) point clouds. The framework includes pre-processing of data, segmenting the wood and foliage at tree level using Weighted Random Forest (WRF) classifier and constructing Quantitative Structure Model (QSM) of the wooden components to estimate its biomass. The flow was extended to AGB estimation of 33 x 33 m plot by integrating tree level framework. The study also finds a unique solution to estimate the contribution of pneumatophores in the AGB. Segmentation of wood/foliage of tree point cloud using WRF yielded better results with an increment of 15.27 % in Balanced accuracy, 0.2 of Cohen's Kappa coefficient, and 7.45 % in F1score than RF classifier. AGB estimation of mangroves using our approach using TLS data is 47.54 T/ha which has a mean bias of 0.0044 T/ha and RMS variation of 0.026 T/ ha when compared with the allometric methods. A Breadth-first graph-search segmentation approach was used to count the pneumatophores, aerial roots seen in few mangrove species ($R^2 = 0.94$ with manual counting) and estimate its contribution to AGB of mangroves which is first of its kind using TLS point cloud. This outcome could also aid future studies in modeling the underlying root network and estimating the below-ground biomass.

1. Introduction

Forest's biomass is the principal indicator of the carbon stock and potential of carbon sequestration of a terrestrial ecosystem (Le Toan et al., 1992). Optical and SAR remote sensing data have been employed extensively to study the structural and biophysical parameters of forests using various regression methods (Leboeuf et al., 2012; Le Toan et al., 1992). However, recent studies on remote sensing based estimation of AGB exhibit noticeable variability in the accuracy on the estimate depending on the forest environment and type of remote sensing data used (Zolkos et al., 2013). Additionally, optical remote sensing can only cover the forests canopy and SAR can penetrate only crown height but not the sub-canopy vegetation contributing greatly to the total AGB of the forest.

Recently, LiDAR technology has shown great potential for forest inventory studies at very high resolutions (Nelson et al., 1988; van Leeuwen and Nieuwenhuis, 2010). Ground based Terrestrial Laser Scanning (TLS) appears to deliver the most detailed and precise characterization of forest structures including understory vegetation. Mangroves have special adaptations like, pneumatophores and stilt roots (structures above the ground that resemble inverted roots and are specifically adapted for gaseous exchange in marshy environments) that also have significant contribution in the AGB estimation (Kauffman and Donato, 2012). We strongly believe that TLS techniques will be able to meet this requirement very efficiently with more accuracy.

In terms of spatial and time complexity, it was observed that the techniques that directly process the point clouds outperformed voxelation methods (Charles et al., 2017; Niemeyer et al., 2013; Sedlacek and Zara, 2009; Wang et al., 2019). The methods that involve abstraction of raw point cloud data into rasterised forms, like multi-view stereo

raster or voxel grids, are view-based (Chen et al., 2016; Pang and Neumann, 2016) and volumetric (Huang and You, 2016; Xu et al., 2018). These techniques, however, lose the inherent geometry of point clouds, making them inefficient. Hence, point clouds were directly processed in this work without any transformation.

To separate wooden points from foliage points, algorithms relying on radiometric features of points (Béland et al., 2014) were found to be largely dependent on sensor-specific characteristics. Whereas, algorithms based on geometric features such as spatial coordinates and their geometry were found to be more robust (Tao et al., 2015) and also proven in combination with shortest path analysis, multiple scaled features etc. (Vicari et al., 2019; Krishna Moorthy et al., 2020; Wang et al., 2020). Review of the specified methods shows that computing geometric features for each point at multiple local neighborhood scales made the classifier invariant to point clouds having highly varying point densities. Thus geometric based features were used in this study to separate wooden from foliage points.

The random forest algorithm reduces overfitting and variance for both pixel-based and voxel-based approaches to classify the foliage, wooden, and ground points. It can be used to combine geometric and radiometric features (Zhu et al., 2018), integrate with XGBOOST classifiers (Wang et al., 2019), and use features derived from clump variance eigenvalues and recursive elimination (Ma et al., 2019). These techniques improve the classification accuracy of point clouds based on satellite data (W. Li et al., 2020), aerial platforms (Xue et al., 2020), UAVs, and mobile (Zeybek, 2021). When classes in a dataset lead to a quantitative imbalance, SMOTE was used to simulate additional samples of the minor dataset (Zulfiker et al., 2021). Sometimes weights are assigned to the classes based on their frequency distribution (Pedregosa et al., 2012).

Of the available methods for individual tree segmentation from laser scans of forests, the region-growing methods (Dalponte and Coomes, 2016; Li et al., 2012; Silva et al., 2016) required that the forest stand be relatively simple with well-spaced near-vertical trees for good performance. They may not perform well on terrestrial laser scans of mangrove forest stands which are characterised by a more complex branching structure and overlapping tree crowns. The graph-cut approach for individual tree segmentation proposed by Yang et al., (2016), was not able to perform satisfactorily on point clouds of complex forest stands with many misclassifications of branches of one tree as that of another. Later, Zhang et al., (2019) proposed a segment-based approach that involved thinning of dense TLS point clouds using the curvature points followed by a connected components segmentation to delineate the individual trees.

When the point clouds are classified, polygonal representation of the tree, called a quantitative structure model (QSM) is constructed from wooden points so that the structural and biophysical parameters of the tree can be reliably measured. (Boudon et al., 2014) developed an algorithm called "PlantScan3D" to generate QSMs by constructing a Branch Structure Graph (BSG) from neighboring points and fitting cylinders to reconstruct the 3D polygonal tree. Landes et al., (2015) developed a tool called 'TreeArchitecture' on output of skeletonization process developed by Cao et al., (2010) to create the tree structure. 'TreeArchitecture' involved the development of Delaunay triangulation and cylinder fitting on the skeletonization. "SimpleTree" is another technique created by Hackenberg et al. (2015) that involves fitting cylinders to the segments of skeletal nodes that are extracted by cutting spheres from the point cloud.

Indian mangroves have been widely studied for the estimation of biophysical parameters such as height, biomass, basal area and Leaf Area Index (LAI) using varied remote sensing data such as multispectral, hyperspectral and microwave data which are purely based on the radiometric and scattering properties of the canopy cover. Vaghela et al., (2021) regressed allometry based biomass against Sentinel 1A Synthetic Aperture Radar (SAR) to model the biomass of Gulf of Kutch mangroves; Spectral indices of EO1 Hyperion hyperspectral data to model the AGB

of Bhitarkanika mangroves (Anand et al., 2020; Prasad and Gnanappazham, 2018). Later, the integration of radiometric properties optical data and geometric properties like height from stereo photogrammetry were found to improve the accuracy (Almeida et al., 2020). Recently Singh et al., (2023) have integrated TLS and ALOS PALSAR to estimate the AGB for a terrestrial forest environment of Uttarakhand. While Indian mangroves are yet to be explored for the potential of TLS in the estimation of AGB in the context of upscaling to aerial or space scale. Based on the above literature survey, the present study aims to develop an end to end pipeline from the segmentation of 3D point cloud of terrestrial laser scans into foliage, wooden and ground points using Random Forest (RF) algorithms followed by the generation of quantitative structure model of the trunks from the classified wooden points for a tree level, plot level including the pneumatophores incorporating graph theory (Adimoolam et al, 2022).

2. Study area and field data collection

2.1. Study area

Maharashtra, the third-largest state in India accounts for a coastal length of 720 km running from North to South (Jagtap et al., 1994). Most of the mangrove forests are spread across the districts of Mumbai City and Mumbai Suburban, Raigad, Ratnagiri, Sindhudurg, and Thane (FSI 2021) accounting to 320 sq.km. The region was experiencing a constant increase in environmental stress due to various anthropogenic activities during the 1980 s to 2010 s (Kulkarni et al., 2010). Later, about 134 sq.km of increase in forest cover was noticed between 2009 and 2019. It is very important to monitor the mangrove forest stock even with increasing trend of the urban environment of Mumbai for the sustainable conservation and management that motivated the present study on estimating the Above Ground Biomass of the mangroves. The area chosen for this study is bounded by the latitudes 19.029080° N to 19.164466° N and the longitudes 72.922204° E to 73.02001° E. This study area is also characterized by extensive adjoining urban cover where the main contributing rivers are the Ulhas and the Vaitarna rivers (Fig. 1).

The study area is dominated by *Avicennia marina*. Other mangrove species in the region include *Avicennia officinalis, Sonneratia apetala, Aegiceras corniculatum, Bruguiera cylindrica, Rhizophora mucronata, Rhizophora apiculata, Excoecaria agallocha* and associated species like *Acanthus ilicifolius, Salvodora persica* (Mugade and Sapkale, 2014). The data used for this study was collected from the mangrove forests of Thane Creek, Mumbai (Fig. 1) to develop the process of biomass estimation.

2.2. Field data collection

The primary data used in this study was acquired from field surveys and terrestrial laser scans of the mangrove forests. Tree level and plot level laser scans of the mangrove forests are acquired using the FARO Focus S 350 (SM1) terrestrial laser scanner (Fig. 2). Two modes of terrestrial laser scans were acquired in this study: (i) Plot level of size 33 m x 33 m (Fig. 3a) from nine scan positions with an average of 80 trees per plot, (ii) individual trees from 3 positions to avoid occlusion (Fig. 3b). Measured Biophysical parameters include (i) diameter at Breast Height (DBH) using measuring tape (ii) height of each tree in the plot using Laser distometer and (iii) wood core specimen from sample trees using a borer and (iv) the total tree count in each plot.

The plots chosen for the study were dominated by *Avicennia marina*. Individual tree scans were taken from three girth classes namely Large (girth greater than 90 cm), Medium (girth between 40——90 cm), and Small (girth between 29.5 – 40 cm) measured at breast height to estimate the above ground biomass. Six white spherical targets were placed inside every plot in such a way that at least four of the six targets were visible from all the scan positions for further registration of the scans.
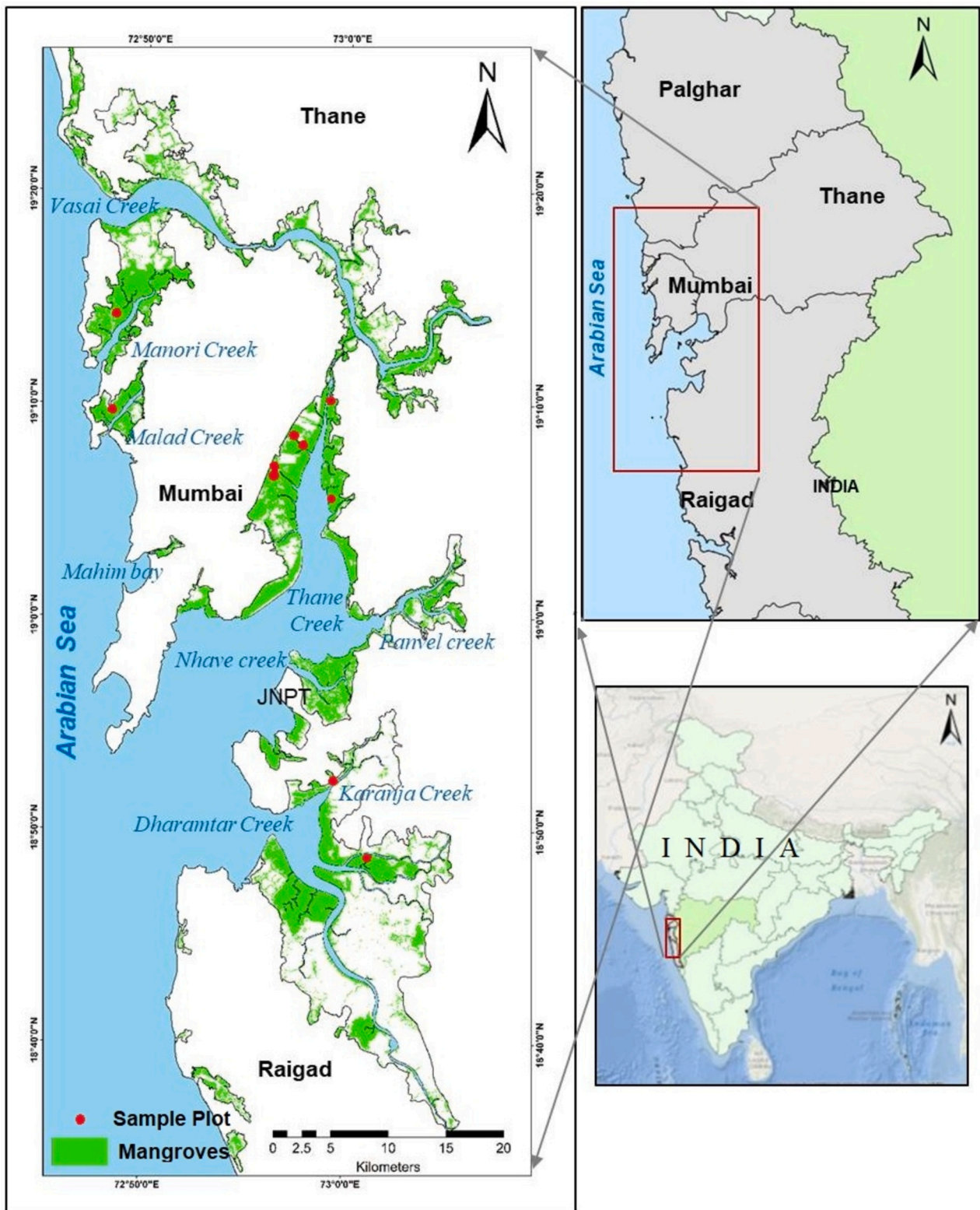
Fig. 1. Study Area showing the mangroves of Mumbai, its surroundings and the sample locations of TLS data collection.

Similarly, fours targets were placed for individual tree scans. These scans were later registered, exported and preprocessed to a single point cloud for both the plot-level and tree-level scans.

3. Methodology

The above-ground biomass (AGB) estimation was carried out through three stages using terrestrial LiDAR scanned data at individual tree levels and for forest plots (Fig. 4).

Fig. 2. Laser scanning using FARO Focus S 350 Terrestrial Laser Scanner.

3.1. Preprocessing of the TLS scans

The TLS scans from each of nine or three scan positions were registered to form the complete point cloud of the tree or plot using automatic target-based registration provided by the FARO SCENE software. This was then converted to ASCII (.xyz) format and further analysed using an open-source *CloudCompare* software.

The resultant point cloud was found to be noisy due to the ghosting effect of moving leaves during scanning. Hence, the point cloud was subjected to a statistical outlier removal tool. The tool computes the average distance of each point to its nearest 'k' neighbours and removes points that are farther than the sum of the average distance and a multiple of the standard deviation. A 'k' value of 6 and a standard deviation multiplier threshold of 1.0 were chosen. The resulting point cloud of a tree or forest plot was filtered for background objects by visual inspection and exported to ASCII format (.xyz) which forms the input for the subsequent stages of the AGB estimation.

3.2. Segmentation

The preprocessed terrestrial LiDAR point cloud data was subjected to segmentation of (i) ground and non-ground points (ii) non-ground points into either wood or foliage points, (iii) Generation of the Quantitative Structure Model (QSM) and (iv) Estimation of the above-ground volume of wooden structure of individual trees and plots. Ground points above the ground were removed using the cloth simulation filter (Zhang et al., 2016) which is commonly used to generate the approximate ground surface for the objects or features when point clouds are absent or very less by inverting the point clouds.

The resultant non-ground point cloud consisted of foliage (leaves) and wooden parts (stem, branches and other wooden components). Points of wooden components are considered the most essential in estimating the AGB as they contribute more than 97 % of the AGB of mangroves (Tran et al., 2017). We used a supervised random forest classifier to classify non-ground point clouds into leaves and wood using a total of 30 features. This includes three eigenvalues (λ_1, λ_2, λ_3) and three zenith angles (θ_1, θ_2, θ_3) of the corresponding eigenvectors of the covariance matrix are computed for each point. These six features were computed at five spatial scales (0.1 m, 0.25 m, 0.5 m, 0.75 m and 1 m) using Python resulting into 30 features (Krishna Moorthy et al., 2020). The covariance matrix for *x* value of 3D points in a neighbourhood (N) is computed from Equation 1 and the azimuth (θ) of the eigenvectors, V can be calculated as in Equation (2).

$$Cov_x \ = \sum_{i=1}^{N}(X_i - \overline{X})(X_i - \overline{X})T \quad (1)$$

$$\theta = \arctan\left(\frac{V_2}{V_1}\right) \quad (2)$$

where, V_1 and V_2 are the first and second elements of the eigenvector respectively.

The scatter plot of the first three features among these (Fig S1) clearly depicts the separability achieved from these features. The plot also shows a class imbalance between the foliage and wooden point clouds as noticed by earlier researchers (Zulfiker et al., 2021). Hence, we used weighted RF classifier also to handle the class imbalance. The weighted random forest classifier is essentially the 'balanced' variant of the standard random forest classifier in the scikit-learn (Pedregosa et al., 2011) python library. This classifier assigns weights to each class inversely proportional to the corresponding class' frequency in the input dataset. To validate the classification results we used the standard classification metrics such as Balanced Accuracy Score, Cohen's Kappa Score, F1 Score and Area under Receiver Operator Characteristics (ROC-AUC) Curve and it was made by performing 10-fold cross-validation on point clouds of ten mangrove trees of large, medium and small diameters which are manually labelled.

3.3. Development of quantitative structure model

After classifying the tree point cloud into leaves and wood, the Quantitative Structure Model (QSM) of the tree was constructed from
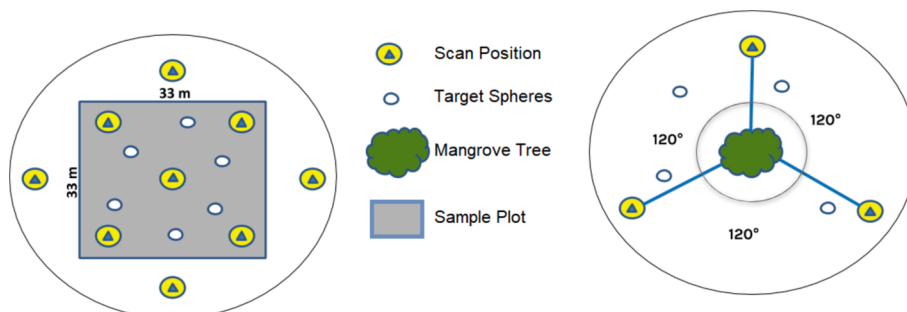

Fig. 3. Multi-station Terrestrial Laser Scanner Survey Layouts of (a) a plot and (b) a single tree.
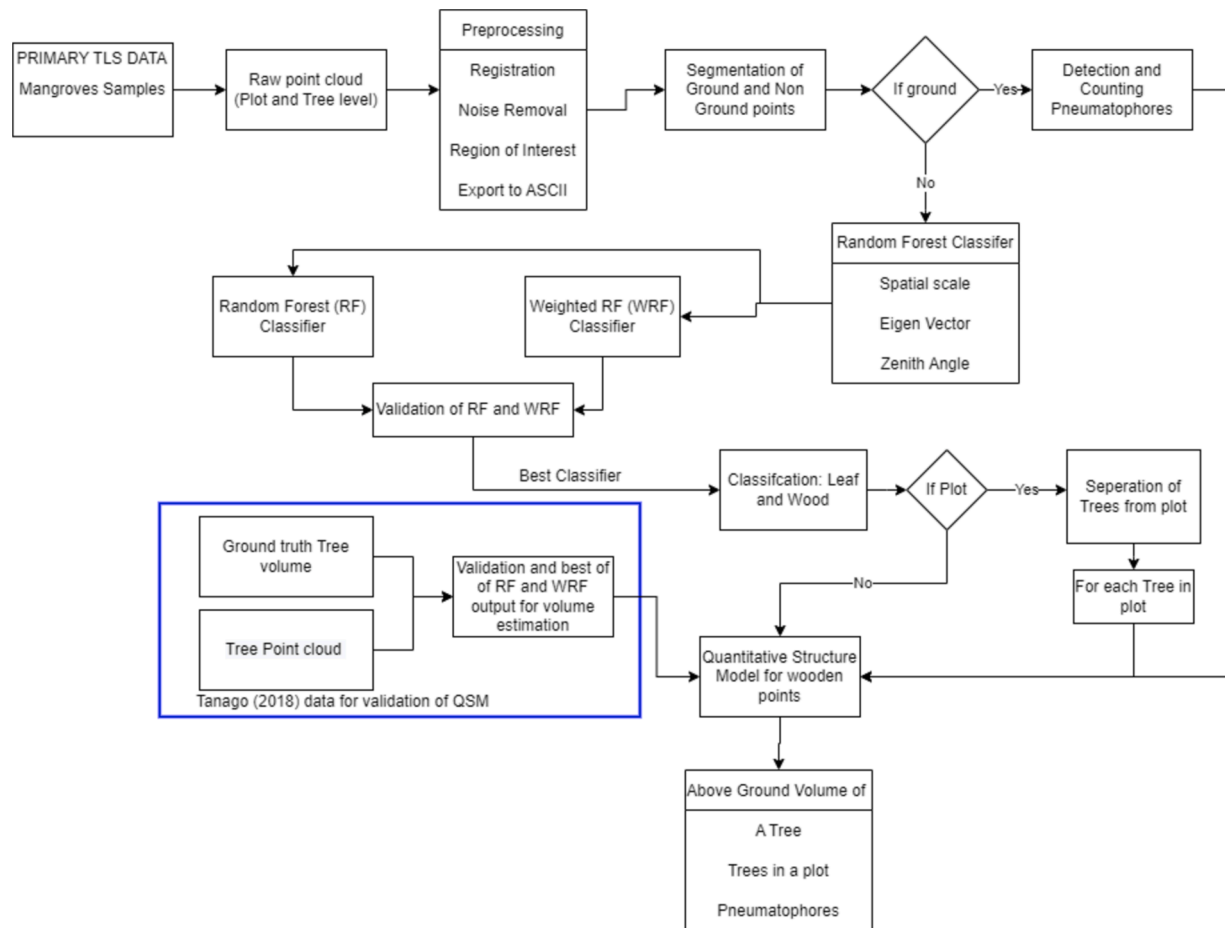
Fig. 4. Methodology of the steps involved in estimating above ground volume of a tree, groups of trees in a plot and pneumatophores.

the wooden points as a hierarchical collection of cylinders using Sim‐pleTree of Computree (Hackenberg et al., 2015). The output of this procedure is a polygonal mesh file accompanied by information such as cylinder descriptions, the volume of the tree, the number of branches in each level of the branching hierarchy, etc. Later, the above-ground biomass of the tree was estimated as a product of the estimated vol‐ume and wood density. The wood density of the tree was obtained by collecting core wood samples of that tree and estimating by a simple oven-drying experimental setup. Our study assumed a uniform density for the tree *A. marina* to calculate AGB as reviewed through the litera‐ture (Fajardo, 2018). The density was estimated as 513 kg/m^3 by col‐lecting wooden core samples collected from 10 trees of varying DBH. The TLS based estimation of AGB was compared against the AGB esti‐mated using conventional allometric methods (Komiyama et al., 2005) (SM2).

3.4. Above-ground biomass estimation of forest plots

Analogous to the estimation of AGB from individual tree point clouds, the ground and non-ground points of the forest plot were sepa‐rated followed by classification of non-ground to wooden and foliage using WRF by deriving geometric features. In addition, a parallel workflow was carried out to segment the pneumatophores and estimate their contribution to AGB of forest plots.

To segment and separate the individual trees from plot-level wooden point clouds, the connected components segmentation tool of *Cloud‐Compare* was used (Lumia et al., 1983). QSM for each tree was con‐structed on the point clouds of the individual trees stored as a polygonal mesh file along with biophysical parameters as explained in section 3.3.

In the case of plot-level point clouds, it is also important to estimate the overall contribution of the pneumatophores to the above-ground biomass of the forest plot. Since, pneumatophores are present just above the ground surface up to a few centimeters height depending on the species type, first, a set of hierarchical layers based on elevation were created from the ground points containing the pneumatophores. These ground points were one of the results of the first segmentation to sepa‐rate the entire point cloud into ground and non-ground point clouds. Then, the layer having the median elevation of 7.5 cm was extracted (it was chosen based on the height of pneumatophores specific to species, in this study it is *Avicennia marina*) and exported as a separate ASCII file. This median layer of the ground points was then converted to an undi‐rected graph. In this graph of median layer ground points, an unlabeled point was selected at random as the root node, a label was assigned to this root node and a breadth-first search was conducted to identify all points connected to the current root node. Based on field observations, a threshold of 3 cm for the horizontal distance between the root node (based on the species *Avicennia marina*) and the visited node was chosen as the connectivity criteria. If a visited node satisfied the connectivity criteria, then it was assigned the same label as the root node. After all the nodes are visited, a new root node from the remaining unlabelled points was chosen and the process was repeated until all points in the input point cloud were assigned a label. The result of this procedure was a point cloud where points belonging to each pneumatophore of the plot were assigned a unique label. To validate the count of pneumatophores by this method, five test patches of size 2 m x 2 m were extracted from across several plots and the pneumatophores in these patches were manually counted. This manually counted number of pneumatophores was used as a reference to validate the estimated count of

pneumatophores.

Once the count of pneumatophores in a plot was obtained with reasonable accuracy, each pneumatophore was modelled as a cone to estimate its volume. The maximum height of each of the segmented pneumatophores is considered as the height of the cone. Since the number of horizontal points was not sufficient to correctly estimate the diameter of each pneumatophore unlike the vertical points for height, the diameter of the cone was chosen based on the in situ sample observations in the plot, as 1 cm. Once the plot level above-ground volume of pneumatophores was obtained using conical construction, the contribution of pneumatophores to AGB at the plot level was calculated as the product of the estimated volume and the wood density 513 kg/m^3 for *Avicennia marina* as mentioned in Sec 3.3.

4. Results

The first set of the study results include (i) registered and pre-processed point clouds of plots (Fig. 5a) and single trees (Fig. 5b) scanned through TLS followed by classification of wood and leaves, and construction of QSMs (Figs. 8 & 9).

4.1. Construction QSM fora tree and a plot

The foliage points in the tree point clouds are filtered from the tree point cloud to improve the accuracy of the tree volume estimates. As the class imbalance between foliage and wood point clouds was evident from the scatter plot of the first three features (Fig. 6), the performance of the RF classifier was compared against a weighted RF classifier and compared using standard accuracy metrics on 10-fold cross validation.

It was observed that there was an average increase of 20 % in the balanced accuracy score, 0.3 in Cohen's Kappa score, 20 % in the ROC AUC score and 21 % in the F1 score when using the weighted RF classifier over the RF classifier (Fig. 6). From these results, it is apparent that the weighted RF classifier performs consistently better than the RF classifier in all cases of foliage vs wood classification and also illustrated by Fig. 6. The visual comparison of classified points using WRF and RF against labelled points of the leaves and the wood of *Avicennia marina* tree (Fig. 7) shows the overestimation of wooden points using RF than

WRF as indicated by circles and arrow in the figure.

After filtering the foliage points from a tree point cloud, the remaining wood points in the point cloud were used to generate a QSM. Since the mangroves are protected and prohibited for destructive sampling, we used bench mark dataset (Gonzalez de Tanago et al., 2018, Figure S2) to validate both the RF and WRF classifiers and used best out of them to generate QSM for mangroves.

These results clearly show that the tree volumes estimated from the weighted RF classifier's results correlate better with the ground truth volumes than do the tree volumes estimated from the RF classifier's results. Based on the accuracy level achieved, the results of the QSM reconstruction of *A. marina* of three DBH (Fig. 8) were used to obtain the total above-ground volume and in turn estimate the above-ground biomass.

It is observed that the misclassified foliage points of RF classifier causing the overestimation of the branches during QSM reconstruction. When the misclassification was reduced by addressing the issue of class imbalance using WRF classifier, the overestimation of branches in the QSMs generated was also reduced and was more representative of the actual tree structure.

4.2. Estimated vs measured structural parameters

The structural parameters estimated from QSM were compared with field measurements. The structural parameter estimation based on TLS point clouds was comparable with the height measured in the field however, it is varied for DBH measurement (Fig. 10). The huge variation in DBH was due to the omission of thin trees during field survey below 0.07 m and a varied number of samples. DBH ranges from 0.08 to 0.29 m and tree height from 5.7 to 9.5 m from field measurements while they range from 0.04 to 0.24 m and 2.6 to 9.8 m respectively from TLS based estimation. As such there are no allometric formulae available to estimate tree volume using height and DBH rather than biomass for mangroves, our comparison is restricted to the tree height and biomass estimation only. From the QSM output of each tree, it was then possible to obtain the above-ground volume of all trees in the plot (0.01 m^3 – 0.53 m^3), which in turn was used to compute the above-ground biomass of the trees with an average wood density of 513 kg/m^3 resulting into an

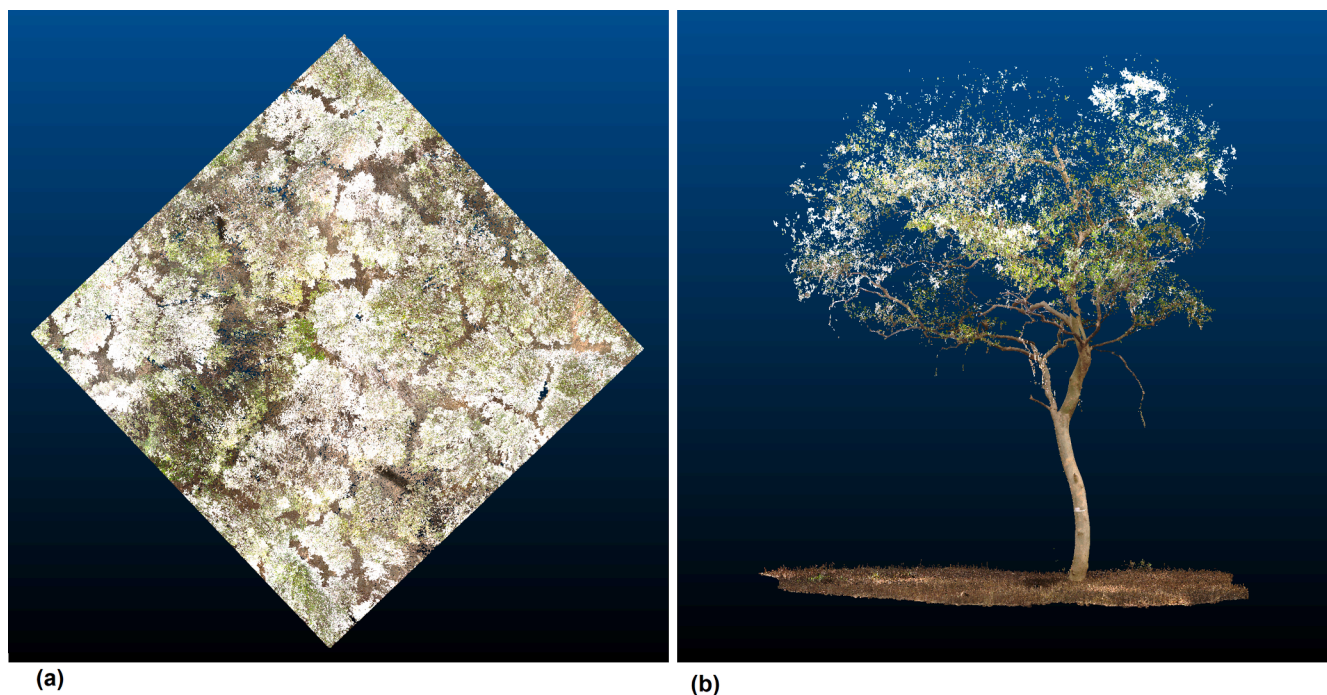**(a)**   **(b)**

Fig. 5. The preprocessed point cloud obtained from TLS scans of (a) top view of a plot of size 33mx33m and (b) a single *A marina* tree of large DBH.
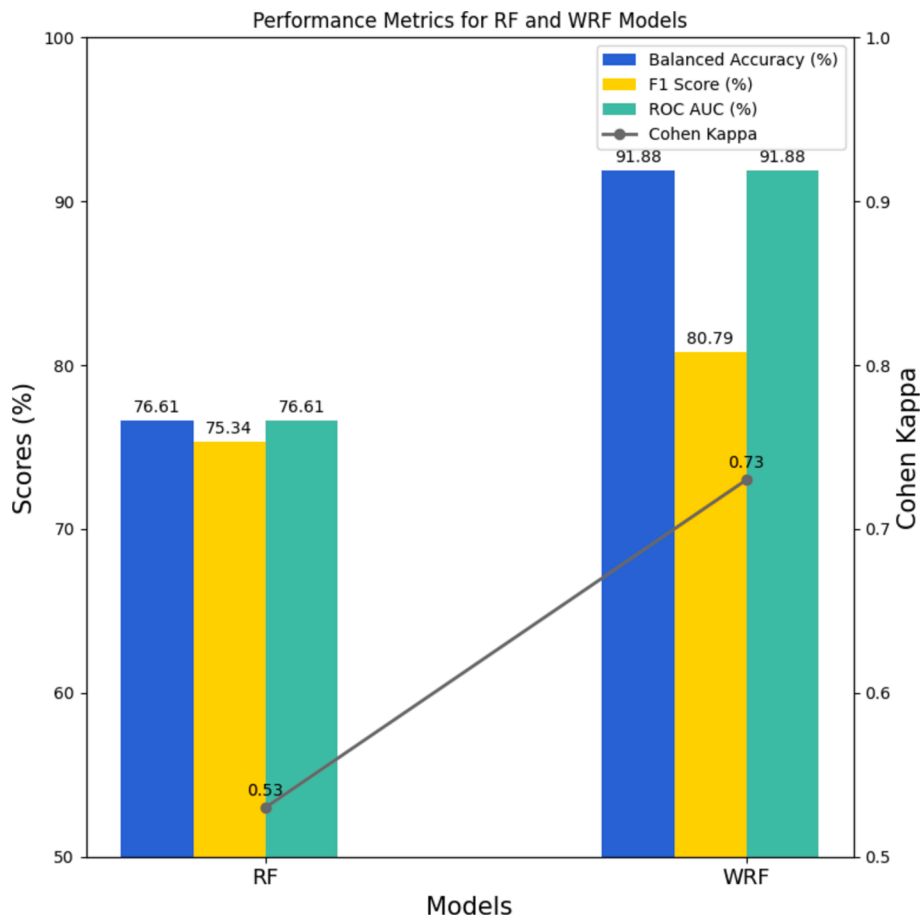
Fig. 6. Balanced Accuracy (%), Cohen's Kappa coefficient, ROC AUC (%) and F1 Scores (%) of RF Classifier vs WRF Classifier.
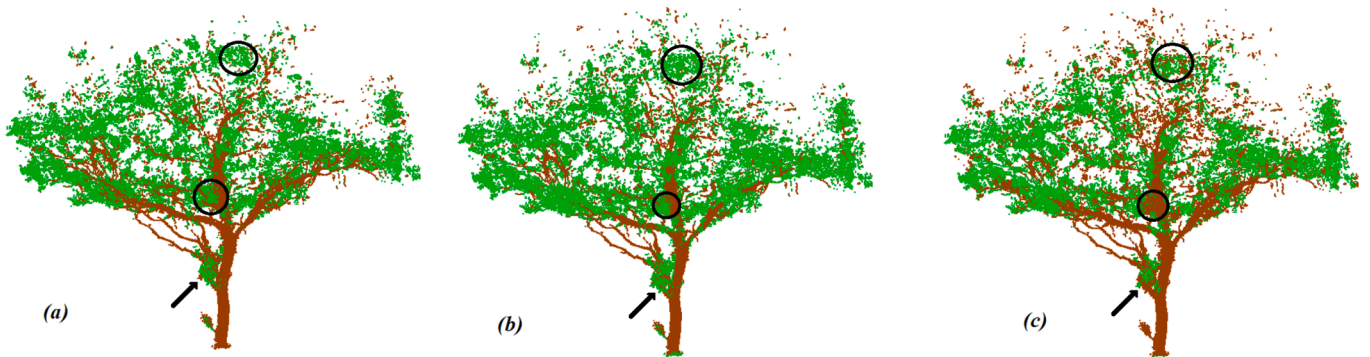

Fig. 7. Labelled Point Cloud of *A. marina* tree (a), Classified output of the same tree using Weighted Random Forest (b) and Random Forest algorithms(c).

average of AGB of 44.11 kg/tree with a range of 2.3–253.89 kg/tree using allometric methods and 46.16 kg/tree with a range of 2.44–276.9 kg/tree using TLS based estimation (Fig. 11). The average density of AGB estimated using allometric and TLS based methods was 42.14 T/ha and 47.54 T/ha respectively.

Furthermore, from the ground points of the plot level point cloud, the contribution of pneumatophores (Fig. 12 a) to plot-level AGB was also calculated. This was done by performing a breadth-first graph search based segmentation of the ground points of the plot-level point cloud, to segment each pneumatophore shown in multiple colors (Fig. 12 b) and obtain their total count from the plot level point cloud (Figure S4)). The results of the estimation of pneumatophores in the forest plot shows an RMSE of 31.5 counts and a best bit of 0.91 between the actual and estimated count. However, there exists a small overestimation of count

that would have been resulted due to the point clouds acquired from closely spaced pneumatophores and omitting few in manual count. Because of the presence of very dense pneumatophores and very few points for each pneumatophore, construction of the QSM from the point clouds was not yielding meaning full result. Hence, each pneumatophore was constructed into a conical shape with a base diameter of 1 cm and the height of each pneumatophore stand measured using segmentation process (Fig. 12. c). The average volume of constructed pneumatophores is estimated as 0.001 m^3/m^2 contributing to increase the AGB density by 5.64 T/ha which is comparable with the estimation of 4.53 T/ha of (Torres et al., 2019).
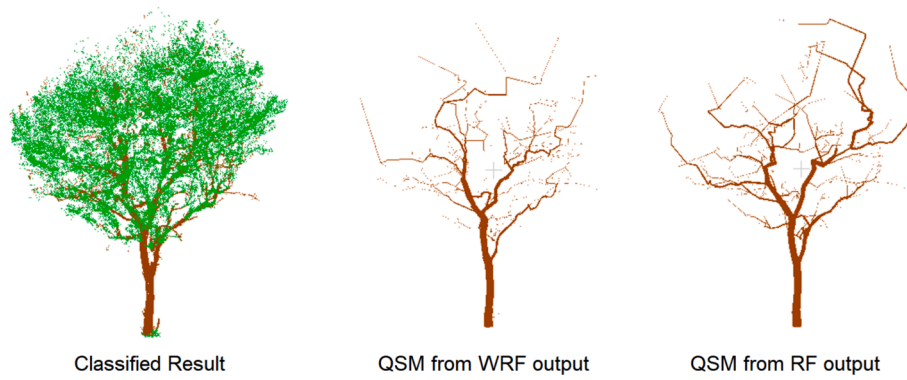
Fig. 8. QSMs of *Avicennia marina* trees generated from points clouds classified using WRF and RF Classifiers.
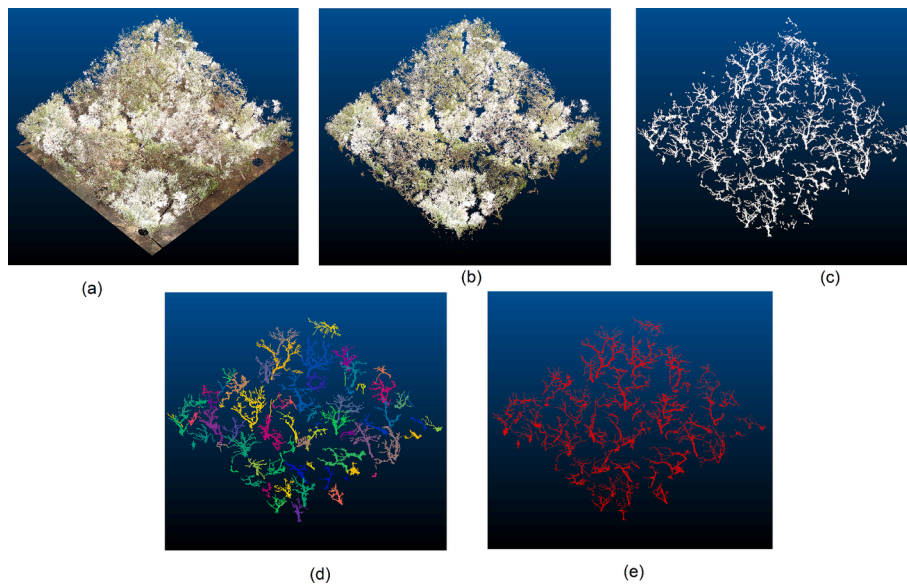

Fig. 9. Point cloud outputs of the Sequence of Steps followed for the estimation of QSM of an entire Forest Plot. (a) Preprocessed. (b) Ground Segmented. (c) Foliage Filtered. (d) Individual Tree Segmentation of the Foliage Filtered (e) QSM Reconstruction of each tree in the Plot.
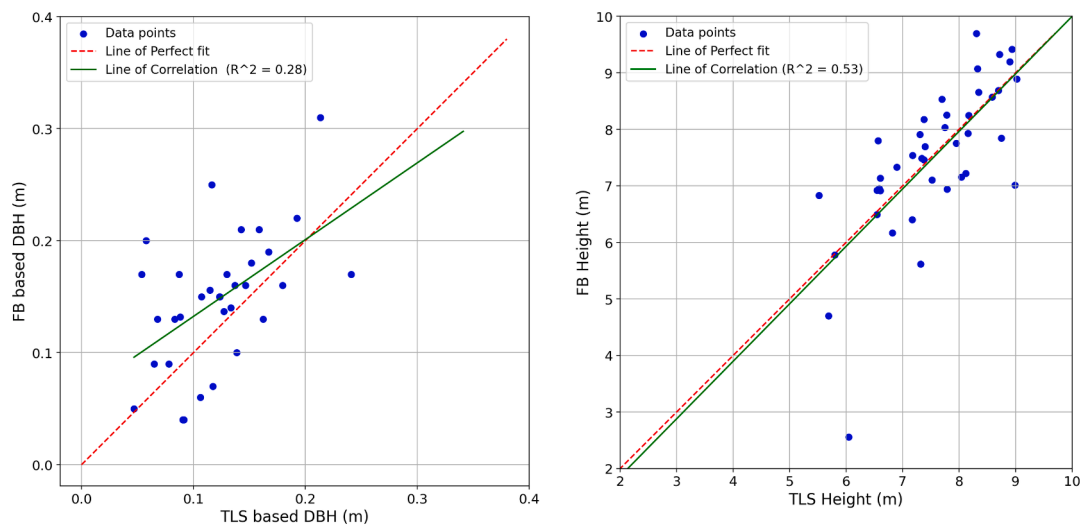

Fig. 10. Comparison of (a) Diameter at Breast Height (DBH) and (b) Height estimated for the trees of sample plot using TLS derived tree structure and the field survey measurements.
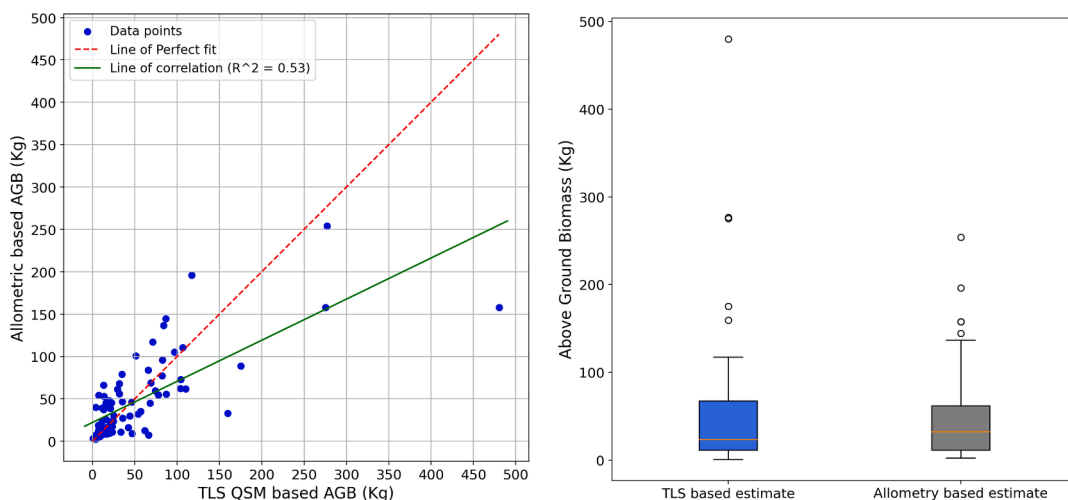
Fig. 11. Comparison of above ground biomass estimated for the sample plot using allometric equation and TLS method using (a) scatter plot and Deviation metrics and (b) box plot chart showing their distribution.
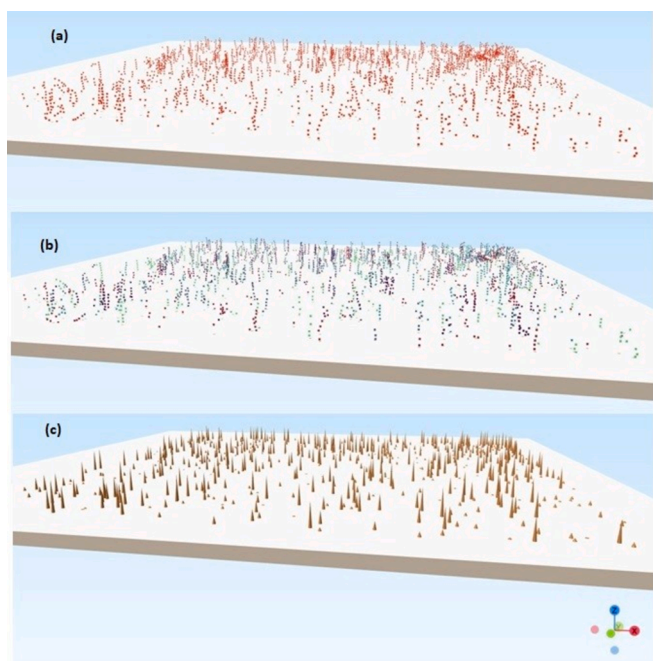

Fig. 12. Detection of Individual Pneumatophores of a Plot (a) Point Clouds of Pneumatophores (b) Individually Segmented Pneumatophores and (c) Constructed pneumatophores.

5. Discussion

The random forest classifier used in this study for foliage filtering performed noticeably better when adding a weight factor to each of the input classes. This is due to the number of foliage points is several times higher than the wood points due to the multifold surface of the leaves.

Above ground volume estimation using the proposed approach resulted with a lesser RMSE for weighted RF classifiers output (1.543 m^3) than RF (2.037 m^3) due to the significant improvement (20 %) in the classification accuracy of weighted RF. The structural parameter estimation based on TLS point clouds was comparable with height measured in the field however, it is varied for DBH measurement. Significant variation in DBH was noticed because thin trees (below 7 cm DBH) were omitted during field survey. While comparing of AGB using allometric equation and TLS approach of our study shows a mean bias of 4.4 kg and

RMS variation of 25.86 kg respectively for the plot. Also it shows a significant correlation between them with the value of 0.53. With the support of concerned authorities, if true biomass are estimated by destructive sampling, the established potential of the techniques could be proved for mangroves also.

Segmentation of individual pneumatophores of the forest plot was successfully carried out from TLS point clouds from the study. This could help in the quantification of pneumatophores and in turn their contribution to above-ground biomass in inventory studies of mangrove forests. Further, the contribution of pneumatophores, especially for the species with large pneumatophores like *Sonneratia apetalla* would be most significant component of above ground biomass (Kauffman and Donato, 2012).. Based on the observations and inferences drawn in this study, further research can be carried out to explore the potential of deep learning algorithms to achieve better results in the leaf vs. wood classification of point clouds, to develop a robust QSM reconstruction including the presence of foliage points in the point cloud. Recent advancements in laser technology enable the accurate and precise field survey that pave way to upscale the satellite and aerial remote sensing in vegetation studies by optimizing the acquisition parameters (Levick et al., 2021).

6. Conclusions

The primary objective of this study was to develop a frame work for the estimation of above-ground biomass (AGB) from the terrestrial LiDAR point clouds of mangrove forests at tree level and plot level. That was successfully met by classifying foliage and woody points using RF and WRF and construction of tree structure of woody points into tree trunk and pneumatophores using 3D polygonal shapes. The accuracy of classifying the point clouds of foliage and wood could be significantly improved using weighted RF algorithm in comparison with RF by assigning weights as balanced variants to overcome the error due to class imbalance. The mangroves of the plots having varying height and overlapping canopy have very noisy point clouds and segmentation of individual trees and QSM construction was challenging part of the study, however, we could get the near real tree distribution using visualization tools. The pipeline developed in this study achieved satisfactory performance on the benchmark dataset also used for validation in this study. The methodology proposed in this study could be generalised to predict the AGB of forest plots of any tree species. This study also proposes a method to estimate the contribution of pneumatophores to AGB, which are specially adapted aerial roots characteristic to mangrove forests that are generally neglected in AGB estimation using point cloud

data. The proposed pipeline will be a pre-runner and would form a baseline ground truth information for the effective utilisation of the recent space borne laser data like GEDI and MOLI for upscaling the biophysical characterization of inaccessible and ecologically important mangrove ecosystem in a larger extent. The use of TLS sampling can expand the options for the calibration and validation of multiple spaceborne LiDAR, SAR, and optical missions in studies over larger area. The development of LiDAR techniques enabled the assessment of three dimensional structure of the tree cover to replicate the actual tree structure for modelling the biophysical parameters as close to real.

CRediT authorship contribution statement

Yeshwanth Kumar Adimoolam: Conceptualisation, Data curation, Methodology, Formal analysis, Investigation, Software, Validation, Writing – original draft. **Nithin D. Pillai:** Data curation, Formal analysis, Investigation. **Gnanappazham Lakshmanan:** Conceptualisation, Methodology, Formal analysis, Investigation, Software, Validation, Supervision, Writing – review, editing & final version.. **Deepak Mishra:** Methodology, Investigation, Supervision, Writing – review & editing. **Vinay Kumar Dadhwal:** Methodology, Visualization, Writing – review & editing, Funding acquisition.

Declaration of competing interest

The authors declare that they have no known competing financial interests or personal relationships that could have appeared to influence the work reported in this paper.

Appendix A. Supplementary data

Supplementary data to this article can be found online at https://doi.org/10.1016/j.ejrs.2024.11.002.

References

Adimoolam, Y.; Pillai, N.D.; Lakshmanan, G.; Mishra, D.; Dadhwal, V.K. Estimation of Above Ground Volume of Mangrove Forest Trees from Terrestrial LiDAR Data using Supervised Machine Learning Algorithms. Preprints 2022, 2022100190. 10.20944/preprints202210.0190.v1.

Almeida, A., Gonçalves, F., Silva, G., Souza, R., Treuhaft, R., Santos, W., Loureiro, D., Fernandes, M., 2020. Estimating structure and biomass of a secondary Atlantic forest in Brazil using fourier transforms of vertical profiles derived from UAV photogrammetry point clouds. Remote Sens. (Basel) 12, 3560. https://doi.org/10.3390/rs12213560.

Anand, A., Pandey, P.C., Petropoulos, G.P., Pavlides, A., Srivastava, P.K., Sharma, J.K., Malhi, R.K.M., 2020. Use of hyperion for mangrove forest carbon stock assessment in bhitarkanika forest reserve: a contribution towards blue carbon initiative. Remote Sens. (Basel) 12, 597. https://doi.org/10.3390/rs12040597.

Béland, M., Baldocchi, D.D., Widlowski, J.-L., Fournier, R.A., Verstraete, M.M., 2014. On seeing the wood for the leaves and the role of voxel size in determining leaf area distribution of forests with terrestrial LiDAR. Agric. Meteorol. 184, 82–97. https://doi.org/10.1016/j.agrformet.2013.09.005.

Boudon, F., Preuksakarn, C., Ferraro, P., Diener, J., Nacry, P., Nikinmaa, E., Godin, C., 2014. Quantitative assessment of automatic reconstructions of branching systems obtained from laser scanning. Ann. Bot. 114, 853–862. https://doi.org/10.1093/aob/mcu062.

Cao, J., Tagliasacchi, A., Olson, M., Zhang, H., Su, Z., 2010. Point cloud skeletons via laplacian based contraction. In: 2010 Shape Modeling International Conference. IEEE, pp. 187–197. https://doi.org/10.1109/SMI.2010.25.

Charles, R.Q., Su, H., Kaichun, M., Guibas, L.J., 2017. PointNet: deep learning on point sets for 3D classification and segmentation. In: 2017 IEEE Conference on Computer Vision and Pattern Recognition (CVPR), pp. 77–85. https://doi.org/10.1109/CVPR.2017.16.

Chen, X., Ma, H., Wan, J., Li, B., Xia, T., 2016. Multi-View 3D Object Detection Network for Autonomous Driving.

Dalponte, M., Coomes, D.A., 2016. Tree-centric mapping of forest carbon density from airborne laser scanning and hyperspectral data. Methods Ecol. Evol. 7, 1236–1245. https://doi.org/10.1111/2041-210X.12575.

Fajardo, A., 2018. Insights into intraspecific wood density variation and its relationship to growth, height and elevation in a treeline species. Plant Biol. 20, 456–464. https://doi.org/10.1111/plb.12701.

Gonzalez de Tanago, J., Lau, A., Bartholomeus, H., Herold, M., Avitabile, V., Raumonen, P., Martius, C., Goodman, R.C., Disney, M., Manuri, S., Burt, A., Calders, K., 2018. Estimation of above-ground biomass of large tropical trees with

terrestrial LiDAR. Methods Ecol. Evol. 9, 223–234. https://doi.org/10.1111/2041-210X.12904.

Hackenberg, J., Spiecker, H., Calders, K., Disney, M., Raumonen, P., 2015. SimpleTree—An efficient open source tool to build tree models from TLS clouds. Forests 6, 4245–4294. https://doi.org/10.3390/f6114245.

Huang, J., You, S., 2016. Point cloud labeling using 3D convolutional neural network. In: 2016 23rd International Conference on Pattern Recognition (ICPR). IEEE, pp. 2670–2675, 10.1109/ICPR.2016.7900038.

Jagtap, T.G., Untawale, A.G., Inamdar, S.N., 1994. Study of mangrove environment of Maharashtra coast using remote sensing data. Indian J. Mar. Sci. 23, 90–93.

Kauffman, J.B., Donato, D., 2012. Protocols for the measurement, monitoring and reporting of structure, biomass and carbon stocks in mangrove forests. 10.17528/cifor/003749.

Komiyama, A., Poungparn, S., Kato, S., 2005. Common allometric equations for estimating the tree weight of mangroves. J. Trop. Ecol. 21, 471–477. https://doi.org/10.1017/S0266467405002476.

Krishna Moorthy, S.M., Calders, K., Vicari, M.B., Verbeeck, H., 2020. Improved supervised learning-based approach for leaf and wood classification from LiDAR point clouds of forests. IEEE Trans. Geosci. Remote Sens. 58, 3057–3070. https://doi.org/10.1109/TGRS.2019.2947198.

Kulkarni, V.A., Jagtap, T.G., Mhalsekar, N.M., Naik, A.N., 2010. Biological and environmental characteristics of mangrove habitats from Manori creek, West Coast, India. Environ. Monit. Assess. 168, 587–596. https://doi.org/10.1007/s10661-009-1136-x.

Landes, T., Saudreau, M., Najjar, G., Kastendeuch, P., Guillemin, S., Colin, J., Luhahe, R., 2015. 3D tree architecture modeling from laser scanning for urban microclimate study. 9th International Conference on Urban Climate Jointly with 12th Symposium on the Urban Environment (ICUC9). France.

Le Toan, T., Beaudoin, A., Riom, J., Guyon, D., 1992. Relating forest biomass to SAR data. IEEE Trans. Geosci. Remote Sens. 30, 403–411. https://doi.org/10.1109/36.134089.

Leboeuf, A., Fournier, R.A., Luther, J.E., Beaudoin, A., Guindon, L., 2012. Forest attribute estimation of northeastern Canadian forests using QuickBird imagery and a shadow fraction method. For. Ecol. Manage. 266, 66–74. https://doi.org/10.1016/j.foreco.2011.11.008.

Levick, S.R., Whiteside, T., Loewensteiner, D.A., Rudge, M., Bartolo, R., 2021. Leveraging TLS as a calibration and validation tool for MLS and ULS mapping of savanna structure and biomass at landscape-scales. Remote Sens. (Basel) 13, 257. https://doi.org/10.3390/rs13020257.

Li, W., Guo, Q., Jakubowski, M.K., Kelly, M., 2012. A New method for segmenting individual trees from the lidar point cloud. Photogramm. Eng. Remote Sens. 78, 75–84. https://doi.org/10.14358/PERS.78.1.75.

Li, W., Niu, Z., Shang, R., Qin, Y., Wang, L., Chen, H., 2020. High-resolution mapping of forest canopy height using machine learning by coupling ICESat-2 LiDAR with Sentinel-1, Sentinel-2 and Landsat-8 data. Int. J. Appl. Earth Obs. Geoinf. 92, 102163. https://doi.org/10.1016/j.jag.2020.102163.

Lumia, R., Shapiro, L., Zuniga, O., 1983. A new connected components algorithm for virtual memory computers. Comput vis Graph Image Process 22, 287–300. https://doi.org/10.1016/0734-189X(83)90071-3.

Ma, Z., Pang, Y., Li, Z., Lu, H., Liu, L., Chen, B., 2019. Fine classification of near-ground point cloud based on terrestrial laser scanning and detection of forest fallen wood. J. Remote Sens. 23, 743–755.

Mugade, N.R., Sapkale, J.B., 2014. A review of mangrove conservation studies in Maharashtra, India. Interna. J. Eng. Techn. Res. (IJETR) 2, 338–341.

Nelson, R., Krabill, W., Tonelli, J., 1988. Estimating forest biomass and volume using airborne laser data. Remote Sens. Environ. 24, 247–267. https://doi.org/10.1016/0034-4257(88)90028-4.

Niemeyer, J., Rottensteiner, F., Soergel, U., 2013. Classification of urban LiDAR data using conditional random field and random forests. In: Joint Urban Remote Sensing Event 2013. IEEE, pp. 139–142. https://doi.org/10.1109/JURSE.2013.6550685.

Pang, G., Neumann, U., 2016. 3D point cloud object detection with multi-view convolutional neural network. In: 2016 23rd International Conference on Pattern Recognition (ICPR). IEEE, pp. 585–590. https://doi.org/10.1109/ICPR.2016.7899697.

Pedregosa, F., Varoquaux, G., Gramfort, A., Michel, V., Thirion, B., Grisel, O., Blondel, M., Müller, A., Nothman, J., Louppe, G., Prettenhofer, P., Weiss, R., Dubourg, V., Vanderplas, J., Passos, A., Cournapeau, D., Brucher, M., Perrot, M., Duchesnay, É., 2012. Scikit-learn: Machine Learning in Python. Journal of Machine Learning Research 12, 2825–2830.

Prasad, K.A., Gnanappazham, L., 2018. Estimation of Above Ground Biomass using High Resolution Multispectral Worldview 2 image. Indian Cartogr. 38, 569–579.

Sedlacek, D., Zara, J., 2009. Graph Cut Based Point-Cloud Segmentation for Polygonal Reconstruction. pp. 218–227. 10.1007/978-3-642-10520-3_20.

Silva, C.A., Hudak, A.T., Vierling, L.A., Loudermilk, E.L., O'Brien, J.J., Hiers, J.K., Jack, S.B., Gonzalez-Benecke, C., Lee, H., Falkowski, M.J., Khosravipour, A., 2016. Imputation of Individual Longleaf Pine (Pinus palustris Mill.) Tree Attributes from Field and LiDAR Data. Can. J. Remote Sens. 42, 554–573. https://doi.org/10.1080/07038992.2016.1196582.

Singh, Arunima, Sunni Kanta Prasad Kushwaha, Subrata Nandy, Hitendra Padalia, Surajit Ghosh, Ankur Srivastava, and Nikul Kumari. 2023. "Aboveground Forest Biomass Estimation by the Integration of TLS and ALOS PALSAR Data Using Machine Learning" Remote Sensing 15, no. 4: 1143.

Tao, S., Guo, Q., Xu, S., Su, Y., Li, Y., Wu, F., 2015. A geometric method for wood-leaf separation using terrestrial and simulated Lidar Data. Photogramm. Eng. Remote Sens. 81, 767–776. https://doi.org/10.14358/PERS.81.10.767.

Torres, J.R., Barba, E., Choix, F.J., 2019. Production and biomass of mangrove roots in relation to hydroperiod and physico-chemicalproperties of sediment and water in the Mecoacan Lagoon, Gulf of Mexico. Wetl. Ecol. Manag. 27, 427–442.

Tran, P., Gritcan, I., Cusens, J., Alfaro, A.C., Leuzinger, S., 2017. Biomass and nutrient composition of temperate mangroves (Avicennia marina var. australasica) in New Zealand. N. Z. J. Mar. Freshw. Res. 51, 427–442. https://doi.org/10.1080/00288330.2016.1260604.

Vaghela, B., Chirakkal, S., Putrevu, D., Solanki, H., 2021. Modelling above ground biomass of Indian mangrove forest using dual-pol SAR data. Remote Sens. Appl. 21, 100457. https://doi.org/10.1016/j.rsase.2020.100457.

van Leeuwen, M., Nieuwenhuis, M., 2010. Retrieval of forest structural parameters using LiDAR remote sensing. Eur. J. For. Res. 129, 749–770. https://doi.org/10.1007/s10342-010-0381-4.

Vicari, M.B., Disney, M., Wilkes, P., Burt, A., Calders, K., Woodgate, W., 2019. Leaf and wood classification framework for terrestrial LiDAR point clouds. Methods Ecol. Evol. 10, 680–694. https://doi.org/10.1111/2041-210X.13144.

Wang, D., Momo Takoudjou, S., Casella, E., 2020. LeWoS: A universal leaf-wood classification method to facilitate the 3D modelling of large tropical trees using terrestrial LiDAR. Methods Ecol. Evol. 11, 376–389. https://doi.org/10.1111/2041-210X.13342.

Wang, Y., Sun, Y., Liu, Z., Sarma, S.E., Bronstein, M.M., Solomon, J.M., 2019. Dynamic graph CNN for learning on point clouds. ACM Trans. Graph. 38, 1–12. https://doi.org/10.1145/3326362.

Xu, Y., Tuttas, S., Hoegner, L., Stilla, U., 2018. Voxel-based segmentation of 3D point clouds from construction sites using a probabilistic connectivity model. Pattern Recogn. Lett. 102, 67–74. https://doi.org/10.1016/j.patrec.2017.12.016.

Xue, D., Cheng, Y., Shi, X., Fei, Y., Wen, P., 2020. An improved random forest model applied to point cloud classification. IOP Conf. Ser.: Mater. Sci. Eng. 768, 072037. https://doi.org/10.1088/1757-899X/768/7/072037.

Yang, B., Dai, W., Dong, Z., Liu, Y., 2016. Automatic forest mapping at individual tree levels from terrestrial laser scanning point clouds with a hierarchical minimum cut method. Remote Sens. (Basel) 8, 372. https://doi.org/10.3390/rs8050372.

Zeybek, M., 2021. Classification of UAV point clouds by random forest machine learning algorithm. Turk. J. Eng. 10.31127/tuje.669566.

Zhang, W., Qi, J., Wan, P., Wang, H., Xie, D., Wang, X., Yan, G., 2016. An easy-to-use airborne LiDAR data filtering method based on cloth simulation. Remote Sens. (Basel) 8, 501. https://doi.org/10.3390/rs8060501.

Zhang, W., Wan, P., Wang, T., Cai, S., Chen, Y., Jin, X., Yan, G., 2019. A novel approach for the detection of standing tree stems from plot-level terrestrial laser scanning data. Remote Sens. (Basel) 11, 211. https://doi.org/10.3390/rs11020211.

Zhu, X., Skidmore, A.K., Darvishzadeh, R., Niemann, K.O., Liu, J., Shi, Y., Wang, T., 2018. Foliar and woody materials discriminated using terrestrial LiDAR in a mixed natural forest. Int. J. Appl. Earth Obs. Geoinf. 64, 43–50. https://doi.org/10.1016/j.jag.2017.09.004.

Zolkos, S.G., Goetz, S.J., Dubayah, R., 2013. A meta-analysis of terrestrial aboveground biomass estimation using lidar remote sensing. Remote Sens. Environ. 128, 289–298. https://doi.org/10.1016/j.rse.2012.10.017.

Zulfiker, M., Ety, N., Biswas, A.A., Nazneen, T., Uddin, M.S., 2021. An in-depth analysis of machine learning approaches to predict depression. Curr. Res. Behav. Sci. 2, 100044. https://doi.org/10.1016/j.crbeha.2021.100044.